Developmental Cell, Vol. 3, 271–282, August, 2002, Copyright ©2002 by Cell Press

ESCRT-III: An Endosome-Associated Heterooligomeric Protein Complex Required for MVB Sorting

Markus Babst,[2] David J. Katzmann, Eden J. Estepa-Sabal, Timo Meerloo, and Scott D. Emr[1]
Department of Cellular and Molecular Medicine and Howard Hughes Medical Institute
School of Medicine
University of California, San Diego
La Jolla, California 92093

Summary

The sorting of transmembrane proteins (e.g., cell surface receptors) into the multivesicular body (MVB) pathway to the lysosomal/vacuolar lumen requires the function of the ESCRT protein complexes. The soluble coiled-coil-containing proteins Vps2, Vps20, Vps24, and Snf7 are recruited from the cytoplasm to endosomal membranes where they oligomerize into a protein complex, ESCRT-III. ESCRT-III contains two functionally distinct subcomplexes. The Vps20-Snf7 subcomplex binds to the endosomal membrane, in part via the myristoyl group of Vps20. The Vps2-Vps24 subcomplex binds to the Vps20-Snf7 complex and thereby serves to recruit additional cofactors to this site of protein sorting. We provide evidence for a role for ESCRT-III in sorting and/or concentration of MVB cargoes.

Introduction

The endosomal system of eukaryotic cells is a complex network of membranous compartments which coordinates protein trafficking between the plasma membrane, the *trans*-Golgi network (TGN), and the vacuole/lysosome (reviewed in Lemmon and Traub, 2000). Two major endosome-to-vacuole/lysosome transport pathways have been described. The biosynthetic pathway delivers newly synthesized proteins from the endoplasmic reticulum (ER) through the Golgi complex and then on to vacuoles/lysosomes via endosomal intermediates. The second pathway is the endocytic pathway, which transports internalized receptors and membrane proteins from the plasma membrane through the endosomal system to the vacuole/lysosome. Therefore, the endocytic and biosynthetic pathways merge within the endosomal system.

Vacuoles/lysosomes play an important role in the degradation of both lipids and cellular proteins. In order to perform this degradative function, vacuoles/lysosomes contain numerous hydrolases which have been transported in the form of inactive precursors via the biosynthetic pathway and are proteolytically activated upon delivery to the vacuole/lysosome. The delivery of transmembrane proteins, such as activated cell surface receptors to the lumen of the vacuole/lysosome, either for degradation/downregulation, or in case of hydrolases, for proper localization, requires the formation of multivesicular bodies (MVBs). These late endosomal structures are formed by invaginating and budding of the limiting membrane into the lumen of the compartment. During this process, a subset of the endosomal membrane proteins is sorted into the forming vesicles. Mature MVBs fuse with the vacuole/lysosome, thereby releasing cargo containing vesicles into its hydrolytic lumen for degradation (Felder et al., 1990; Futter et al., 1996; van Deurs et al., 1993). Endosomal proteins that are not sorted into the intralumenal MVB vesicles are either recycled back to the plasma membrane or Golgi complex, or remain in the limiting membrane of the MVB and are thereby transported to the limiting membrane of the vacuole/lysosome as a consequence of fusion. Therefore, the MVB sorting pathway plays a critical role in the decision between recycling and degradation of membrane proteins.

A well-studied example of MVB-dependent sorting in mammalian cells is the downregulation of activated cell surface receptors (reviewed in Sorkin, 1998). Similarly, yeast cells which have been exposed to α factor pheromone rapidly endocytose the activated G protein-coupled pheromone receptor Ste2, and sort the receptor into the MVB pathway for degradation in the vacuolar lumen (Hicke, 1997; Odorizzi et al., 1998). Furthermore, a cargo of the yeast biosynthetic pathway has been identified which is transported via the MVB sorting pathway into the lumen of the vacuole. The vacuolar enzyme carboxypeptidase S (CPS) is synthesized as a membrane-bound precursor (pro-CPS) which is sorted into vesicles of forming MVBs (Odorizzi et al., 1998; Spormann et al., 1992). Upon delivery of these vesicles to the vacuolar lumen, pro-CPS is proteolytically clipped from its transmembrane domain, resulting in the active soluble form of the enzyme. Recent studies of CPS trafficking revealed that monoubiquitination of the short cytoplasmic tail of pro-CPS is required for efficient sorting of the protein into the MVB pathway (Katzmann et al., 2001; Reggiori and Pelham, 2001). Ubiquitination of cell surface receptors in both yeast and mammalian cells also has been shown to play a role in the downregulation of these proteins via the MVB pathway. Therefore, ubiquitination of both biosynthetic and endocytic cargo serves as a signal for sorting of these proteins into the MVB pathway.

At the endosome, ubiquitinated pro-CPS binds to the protein complex ESCRT-I (endosomal sorting complex required for transport), which initiates its sorting into the MVB vesicles (Katzmann et al., 2001). The genes encoding the three ESCRT-I subunits, Vps23, Vps28, and Vps37, belong to a group of 15 genes called the class E vacuolar protein sorting (*VPS*) genes, which have been shown to be essential for the formation of MVBs (Babst et al., 2000; Katzmann et al., 2001; Odorizzi et al., 1998). Deletion of any of the class E *VPS* genes

[1] Correspondence: semr@ucsd.edu
[2] Present address: MicroGenomics Inc., 5935 Darwin Court, Carlsbad, California 92008.

results in accumulation of endosomal cargoes in large aberrant endosomal structures called class E compartments (Piper et al., 1995; Raymond et al., 1992), as well as mislocalization of MVB cargo to the limiting membrane of the vacuole. In addition to the ESCRT-I subunits, the set of class E Vps proteins also includes Vps22, Vps25, and Vps36, which form the protein complex ESCRT-II (Babst et al., 2002). Vps4 assembles into an AAA-type ATPase, which catalyzes the release of other class E Vps proteins from the endosomal membrane (Babst et al., 1997, 1998, 2002). Mammalian homologs to several of the yeast class E *VPS* genes have been identified, and their analysis suggested that the function of the class E Vps proteins is conserved among all eukaryotes (Babst et al., 2000; Bishop and Woodman, 2000, 2001; Scheuring et al., 1999; Yoshimori et al., 2000).

This study focuses on the four class E Vps proteins Vps2, Vps20, Vps24, and Snf7 (allelic to *VPS32*, hereafter referred to as *SNF7*). These coiled-coil-containing proteins are recruited from the cytoplasm to an endosomal compartment where they oligomerize into a membrane-associated complex called ESCRT-III. We provide evidence that is consistent with a role for this protein complex in cargo concentration and sorting, ultimately resulting in entry of the cargo into the invaginating vesicles of the MVB.

Results

Analysis of the class E Vps proteins Vps24 and Snf7 demonstrated that these proteins are part of an endosome-associated protein complex (Babst et al., 1998). To identify additional proteins in this complex, we tested the remaining class E *vps* mutants for impaired formation of the Vps24-Snf7 protein complex. These studies led to the identification and cloning of two additional class E *VPS* genes, *VPS2* (allelic to *DID4*, *GRD7*, and *REN1*; SGD ORF YKL002W, hereafter referred to as *VPS2*) and *VPS20* (SGD ORF YMR077C), a gene found to be required for transport of the plasma membrane protein Ste6 to the vacuole (Kranz et al., 2001). *VPS2* and *VPS20* encode small hydrophilic proteins which display homology to Vps24 (52% similarity) and Snf7 (47% similarity), respectively. These four proteins all share several common features, including coiled-coil motifs and an N-terminal region enriched in basic amino acids (pI ~10), whereas the C terminus is strongly acidic (pI ~4; Figure 1A).

Consistent with the phenotype of other class E *vps* mutants, deletion of *VPS2* or *VPS20* results in missorting of the vacuolar hydrolases CPY and CPS (see below) and accumulation of endocytic markers (e.g., Ste2 and the hydrophilic dye FM4-64; data not shown) in a large prevacuolar structure, the class E compartment. For further characterization of these proteins, we constructed functional C-terminal hemagglutinin (HA) epitope fusion for both Vps2 and Vps20. Western blot analysis of cells expressing Vps2-HA or Vps20-HA revealed a specific band at ~40 kDa for both proteins which is approximately 10 kDa higher than expected for each of these ORFs (Figure 1B). Similarly, Snf7 and Vps24 have been found to migrate on SDS-PAGE at higher molecular weights than expected (Figure 1B; Babst et al., 1998). However, bacterially expressed Snf7 protein also migrates in an identical manner, suggesting that the size discrepancy is not the result of protein modifications, but rather represents an intrinsic property of the protein (e.g., highly charged nature; Figure 1C, lane 3).

Subcellular fractionation of cells expressing the fusion proteins revealed that 60%–70% of Vps2-HA and Vps20-HA as well as both Vps24 and Snf7 were found in the soluble cytoplasmic fraction (Figure 2A, lanes 1 and 2, 9 and 10, and 17 and 18; Vps2-HA, data not shown). To analyze the oligomeric state of the four small coiled-coil proteins in solution, we determined the native molecular weight of these proteins by gel filtration analysis of yeast cell extracts. The resulting data indicated a molecular weight for the soluble proteins between 40 kDa and 60 kDa (Figure 1B) which, based on the calculated molecular weight of approximately 30 kDa, could suggest that the proteins form homo- or heterodimeric complexes. We therefore analyzed mutant cell extracts by gel filtration and found that the deletion of each of the small coiled-coil proteins did not affect the native molecular weight of soluble Vps24 or Snf7. This suggests that the small coiled-coil proteins do not associate with each other in solution (Figure 1B). To test the possibility of homodimer formation, we expressed a functional $(His)_6$-Snf7 fusion protein in wild-type cells ("L", Figure 1C) and purified the $(His)_6$-tagged protein by Ni^{2+} affinity chromatography. The Western blot analysis of the eluted fraction ("E", Figure 1C) revealed that we enriched only for $(His)_6$-tagged but not endogenous Snf7 protein, which indicated that Snf7 is not present in a homooligomeric complex. Additionally, when expressed in *E. coli*, $(His)_6$-Snf7 eluted from the gel filtration column in the same size range as found for Snf7 from yeast extracts (Figure 1B). Together, the data suggest that in the cytoplasm, the small coiled-coil proteins are monomeric. The higher molecular weights of the small coiled-coil proteins observed by gel filtration might be due to a nonglobular shape of the protein.

Vps2, Vps20, Vps24, and Snf7 Form the Protein Complex ESCRT-III

The cytoplasmic pool of Vps24 and Snf7 transiently associates with an endosomal compartment, and the dissociation and solubilization of these proteins requires the AAA-type ATPase Vps4 (Babst et al., 1998). Consistent with these data and the fractionation presented in Figure 2A, we observed by immunofluorescence microscopy that both Vps2-HA and Vps20-HA are mainly localized to the cytoplasm in wild-type cells (data not shown), but accumulate on large perivacuolar structures, the class E compartments, in a *vps4*Δ strain (Figure 2B). In addition, coimmunostaining with antibodies specific for Vps20-HA or Vps2-HA, and Snf7 (Figure 2B) or Vps24 (Supplemental Figure S1, available at http://www.developmentalcell.com/cgi/content/full/3/2/271/DC1) revealed that all four coiled-coil proteins colocalize in *vps4*Δ cells to the same endosomal compartment. To support the localization data obtained by immunofluorescence microscopy, we performed subcellular fractionations of wild-type and *vps4*Δ cells. We spheroplasted and lysed the yeast cells and separated the

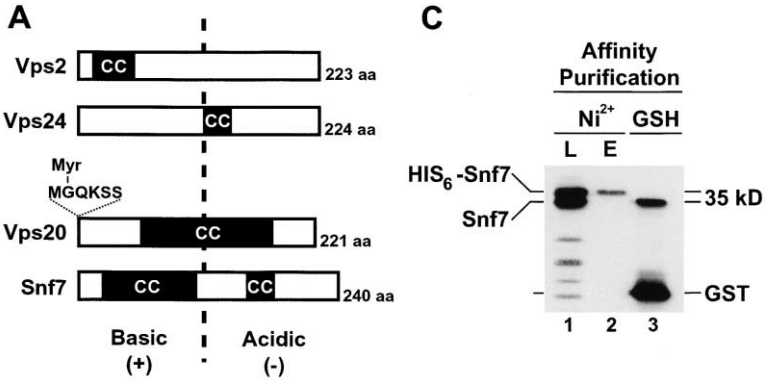

B

	Source	Calculated MW	SDS-PAGE MW	Gel filtration MW
Vps2-HA	wild-type	29.6 kD (25.2)*	~40 kD	49 kD
Vps20-HA	wild-type	30.1 kD (25.6)*	~40 kD	47 kD
Vps24	wild-type	26.2 kD	~35 kD	42 kD
Snf7	wild-type	27.0 kD	~35 kD	59 kD
Snf7	*vps2*Δ	27.0 kD		59 kD
Snf7	*vps20*Δ	27.0 kD		59 kD
Vps24	*snf7*Δ	26.2 kD		42 kD
His_6-Snf7	*E. coli*	28.0 kD		63 kD

Figure 1. ESCRT-III Protein Domain Structures and Molecular Mass Characterization

(A) Domain structure of the class E Vps proteins Vps2, Vps24, Vps20, and Snf7. Putative coiled-coil domains are marked with black boxes. The dashed line divides the proteins by their positively charged N-terminal and negatively charged C-terminal domains. The myristoylation acceptor site for Vps20 is also indicated.

(B) Molecular weight of the small coiled-coil proteins determined by SDS-PAGE or gel filtration analysis. Cell extracts from the indicated strain were subjected to SDS-PAGE and Western blotting or gel filtration analysis (Sephacryl S-100) and the results are presented in table format.

(C) Western blot analysis of Snf7 purified from yeast or bacterial cells. Cellular extract from wild-type yeast expressing $(His)_6$-tagged Snf7 was loaded onto an Ni^{2+} affinity column. The column was washed and the bound proteins were eluted with imidazole-containing buffer. Samples of the loaded extract (L) and the eluted proteins (E) were analyzed by Western blot. The fusion protein GST-Snf7 was expressed in *E. coli* and purified by glutathione (GSH) affinity chromatography. The resulting fraction was incubated with thrombin to cleave the fusion protein between the GST and Snf7 moieties and was analyzed by Western blot (lane 3).

resulting extract by centrifugation at 13,000 × g into soluble and membrane-bound pelletable fractions. These fractions were then analyzed by Western blot for the relative concentration of the coiled-coil proteins. As expected from the microscopy data presented in Figure 2B, we observed for both Vps24 and Snf7 a strong shift into the pelletable pool from ~30% in wild-type to more than 90% in *vps4*Δ cells (Figure 2A, lane 2 compared to 4 and lane 10 compared to 12). However, the Vps4-dependent redistribution was less pronounced for Vps20-HA (Figure 2A, lane 18 compared to 20) and only minimal for Vps2-HA (data not shown). This could be a result of partial dissociation of these proteins from the endosomal membrane during the fractionation procedure, or that the 2- to 3-fold overexpression of the plasmid-encoded Vps2-HA and Vps20-HA might lead to an overrepresentation of these proteins in the soluble fraction.

The colocalization of the four coiled-coil proteins could indicate that they assemble on the endosomal membrane into a protein complex. To test this possibility, we performed immunoprecipitations under native conditions from either the soluble or detergent-solubilized membrane fraction using antibodies specific for one of the coiled-coil proteins. The resulting samples were analyzed by Western blot for the presence of other class E Vps proteins. Taken together, these experiments demonstrated that Vps24 and Snf7 coimmunoprecipitate with either Vps2-HA or Vps20-HA from the membrane-bound fraction of wild-type cells (Figure 2C, lanes 1 and 5). These data, together with the observation that the Vps2-Vps20 interaction is dependent on Vps24 (see below), suggest that the four coiled-coil proteins physically interact when localized to the endosomal membrane. We named the endosome-associated protein complex formed by Vps2, Vps20, Vps24, and Snf7, ESCRT-III, for "endosomal sorting complex required for transport." In contrast, we were not able to observe interactions between the coiled-coil proteins from the cytoplasmic pool (data not shown, but this is consistent with data presented in Figures 1B and 1C). In cells deleted for *VPS4*, we observed a dramatic increase in the formation of ESCRT-III in the membrane-bound fraction (Figure 2C, lanes 2 and 6) which is consistent with the endosomal accumulation of the coiled-coil proteins found in these mutant cells (Figure 2B).

After centrifugation of detergent-solubilized membranes at 100,000 × g, both Vps24 and Snf7 are found in the pellet fraction, suggesting that ESCRT-III is a very large protein complex and thus contains numerous copies of each subunit (Babst et al., 1998). To analyze the subunit composition of ESCRT-III, we performed native immunoprecipitation experiments from cells expressing either *VPS2-HA* or *VPS20-HA*. Using antibodies specific for Vps24 (Figure 2D) or Snf7 (data not shown), we were able to coimmunoprecipitate similar amounts of Vps2-HA and Vps20-HA, suggesting that ESCRT-III contains similar numbers of each of the four coiled-coil proteins. Using high copy plasmids, we overexpressed Snf7 or Vps24 and performed immunoprecipitations using antibodies specific for Vps20 (Figure 2E). The data demonstrated that overexpression of a single coiled-coil protein does not result in elevated levels of this subunit within the ESCRT-III protein complex, suggesting that ESCRT-III has a defined subunit stoichiometry. However, because of the apparent large molecular size of the protein complex, we were not able to determine whether ESCRT-III contains a defined number of subunits.

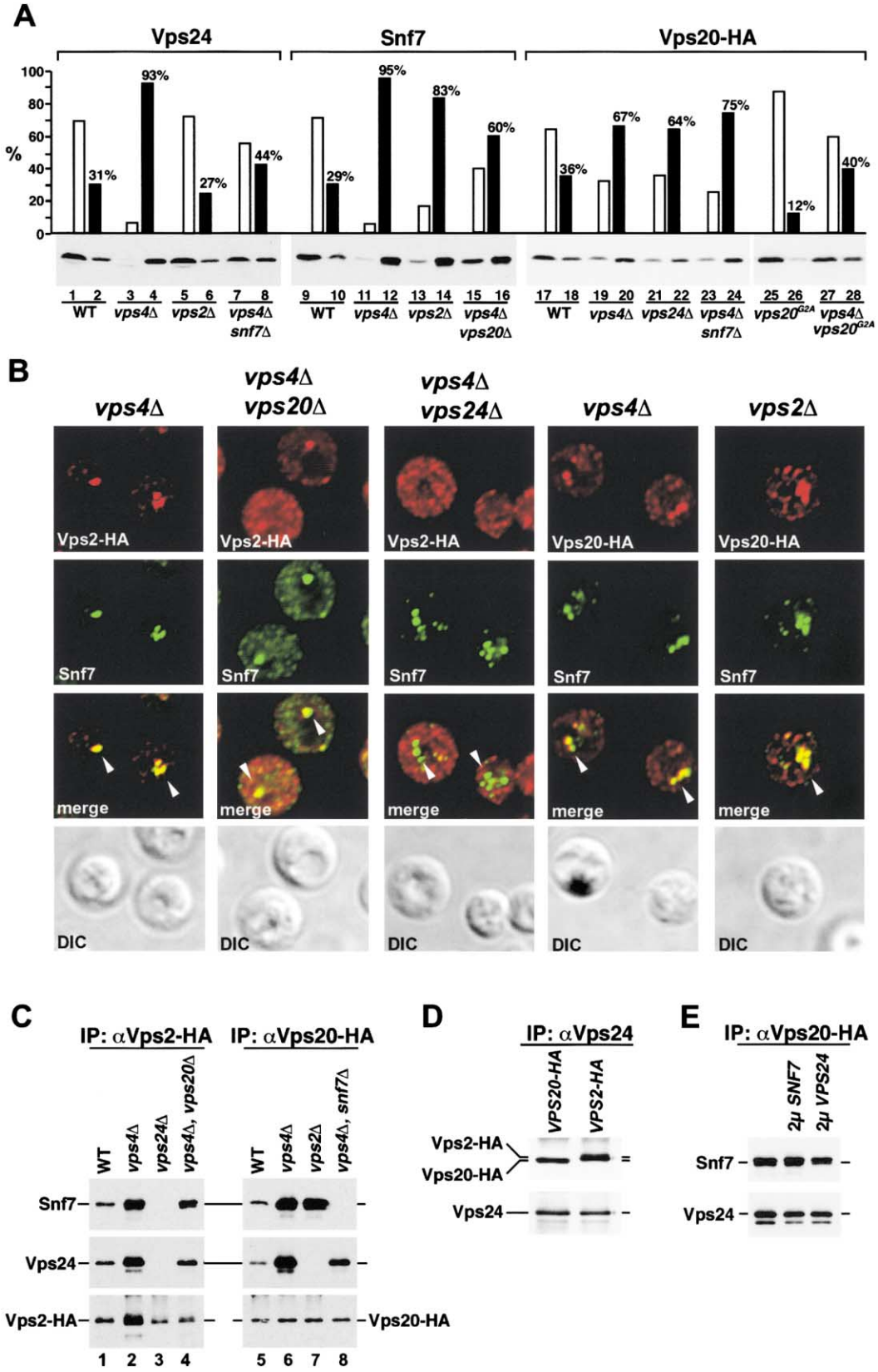

Figure 2. Formation and Membrane Association of ESCRT-III in Wild-Type and Mutant Yeast Strains

(A) Yeast cells were lysed and the resulting extracts were separated by centrifugation at 13,000 × g into soluble fraction (white bars) and membrane-bound (black bars) pellet fractions. These fractions were analyzed by Western blot and quantified using the Scion Image program (Wayne Rasband, NIH).

ESCRT-III Contains Two Functionally Distinct Subcomplexes

Further analysis of the protein interactions within ESCRT-III indicated that this protein complex contains two functionally distinct substructures formed by the two homologous pairs of Vps proteins, Vps2-Vps24 and Vps20-Snf7. Immunofluorescence microscopy, subcellular fractionation, and immunoprecipitation experiments revealed that deletion of either *VPS2* or *VPS24* resulted in accumulation of Snf7 and Vps20 on the endosomal membrane, similar to the accumulation observed in *vps4*Δ cells (Figure 2B; Figure 2A, lanes 13 and 14, and lanes 21 and 22, respectively), suggesting that the Vps2-Vps24 subcomplex is required for the Vps4-dependent dissociation of ESCRT-III. Using an ATPase-defective mutant form of Vps4 (Vps4^{E233Q}), we demonstrated that the ATP-bound form of Vps4 associates with endosomal structures and colocalizes with Snf7 and Vps24 (Babst et al., 1998). We found by immunofluorescence microscopy that the endosomal localization of Vps4^{E233Q} requires the presence of both Vps2 (Figure 3A) and Vps24 (data not shown). Furthermore, it has been shown that the recruitment of Vps4 to the endosome requires its N-terminal coiled-coil domain (Babst et al., 1998). Together, the data suggest that Vps4 binds to ESCRT-III via coiled-coil interactions with the Vps2-Vps24 subcomplex and that this interaction is necessary for the Vps4-dependent dissociation of ESCRT-III.

Further analysis of the *VPS2* and *VPS24* deletion strains revealed that the endosomal association of Vps2 is dependent on the presence of Vps24, and vice versa. Immunofluorescence microscopy of *vps4*Δ cells demonstrated colocalization of Vps2 and Snf7 at endosomal structures. However, in cells that were additionally deleted for *VPS24*, the Vps2 protein showed a cytoplasmic staining with only minimal colocalization with the endosome-associated Snf7 (Figure 2B). It should be noted that the slightly "clumpy" pattern seen for cytosolic staining is an artifact of the fixation procedure and does not represent membranous compartments. Consistent with this observation, coimmunoprecipitation experiments with *vps24*Δ cells indicated a complete loss of interaction between Vps2 and Snf7 (Figure 2C, lane 3). Similarly, deletion of *VPS2* resulted in loss of interaction between Vps24 and the Vps20-Snf7 subcomplex (Figure 2C, lane 7). These data indicate that both Vps2 and Vps24 must be present for proper association with Vps20-Snf7 during ESCRT-III assembly.

Deletion of either *VPS20* or *SNF7* strongly affected the association of the Vps2-Vps24 subcomplex with endosomal membranes. This was demonstrated by immunofluorescence microscopy, which showed in comparison to *vps4*Δ cells a partial redistribution of Vps2 from the class E compartment to the cytoplasm in a *vps4*Δ *vps20*Δ double mutant strain (Figure 2B). Consistent with this, we found by fractionation analysis a loss of the membrane-bound Vps24 pool in both the *vps4*Δ*vps20*Δ (data not shown) and the *vps4*Δ*snf7*Δ strain (Figure 2A, lanes 7 and 8). These data suggested that the Vps20-Snf7 subcomplex is responsible for the membrane association of ESCRT-III. Deletion of one of the Vps20-Snf7 subunits did not block the association of Vps2-Vps24 with the remaining Vps20-Snf7 subunit, which suggested that the Vps2-Vps24 subcomplex is able to interact with either Vps20 or Snf7 independently (Figure 2C, lanes 4 and 8).

Membrane association of Snf7 was partially lost in cells deleted for *VPS20* (Figure 2A, lanes 15 and 16; Figure 2B), whereas deletion of *SNF7* did not decrease the membrane-bound pool of Vps20 (Figure 2A, lanes 23 and 24). Vps20 contains a recognition sequence for the myristoyl-CoA:protein *N*-myristoyltransferase Nmt1,

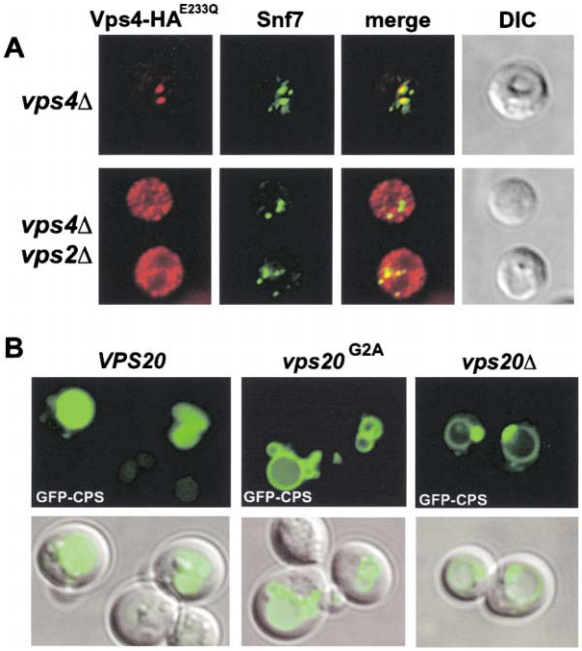

Figure 3. Proper Localization of Vps4 and GFP-CPS Requires ESCRT-III Function

(A) The yeast mutants *vps4*Δ or *vps2*Δ*vps4*Δ were spheroplasted, fixed, and stained with antibodies specific for the HA tag and Snf7. The cells were analyzed by fluorescence and DIC microscopy.

(B) *N*-myristoylation of Vps20 is required for efficient sorting of GFP-CPS into the lumen of the vacuole. The localization of GFP-CPS in either wild-type (*VPS20*) or mutant (*vps20*^{G2A} and *vps20*Δ) yeast cells studied by fluorescence and DIC microscopy.

(B) Requirement of ESCRT-III subunits for the endosomal localization of Vps2 and Vps20 analyzed by immunofluorescence microscopy. Mutant yeast cells expressing *VPS2-HA* or *VPS20-HA* were spheroplasted, fixed, and stained with antibodies specific for the HA tag and Snf7. White arrowheads mark class E compartments.

(C–E) Detergent-solubilized membranes of wild-type and mutant yeast cells expressing either *VPS2-HA* or *VPS20-HA* were subjected to immunoprecipitation experiments under native conditions using antibodies specific for the HA tag (IP: αVps2-HA; IP: αVps20-HA). The resulting samples were analyzed by Western blot for the presence of ESCRT-III subunits as indicated. Detergent-solubilized membranes from *vps4*Δ mutant cells expressing Vps2-HA or Vps20-HA (D) or overexpressing Snf7 or Vps24 (E) were subjected to immunoprecipitation experiments under native conditions using antibodies specific for Vps24 (αVps24). The resulting samples were analyzed by Western blot for the ESCRT-III subunits as indicated.

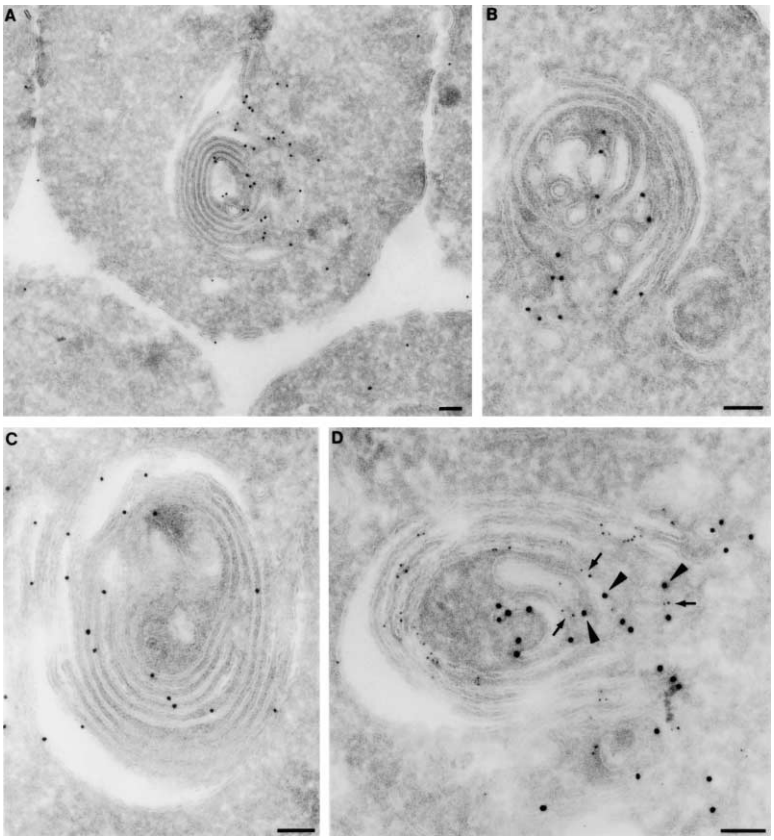

Figure 4. Colocalization of Snf7 (ESCRT-III) and the MVB Cargo GFP-CPS within the Class E Compartment

Cells expressing GFP-CPS and deleted for *VPS4* were prepared for immunoelectron microscopy and labeled with antibodies specific for GFP and/or Snf7.

(A) Characteristic morphology of class E compartment labeled with anti-Snf7 antibody (10 nm gold particles).

(B) Membrane structures within a class E compartment showing single label (10 nm gold) for Snf7.

(C) Typical multilamellar aspect of class E compartment showing single label (10 nm gold) for GFP-CPS. (D) Double-label experiment using 5 nm gold particles (arrows) to detect GFP-CPS and 10 nm (arrowheads) to detect Snf7. All scale bars represent 100 nm.

which during translation covalently attaches myristate to the N-terminal glycine of target proteins. In vitro myristoylation assays demonstrated that an octapeptide derived from the N-terminal sequence of Vps20 is a substrate for Nmt1, suggesting that in yeast, Vps20 is modified by the attachment of the fatty acid myristate (Ashrafi et al., 1998). We mutated the N-terminal glycine of Vps20 to alanine to test whether the lipid modification is required for proper localization and membrane association of Vps20. Fractionation of wild-type cells expressing the $Vps20^{G2A}$ showed an almost complete loss of membrane association (Figure 2A, lanes 25 and 26). However, in cells deleted for the Vps4 ATPase, $Vps20^{G2A}$ accumulated in the membrane fraction, although to a lesser extent than observed with the wild-type protein (compare lanes 19 and 20 with lanes 27 and 28 in Figure 2A).

To address the effect of mutation of the putative myristoylation site in Vps20 on sorting at the MVB, we analyzed trafficking of the MVB cargo CPS in yeast expressing $Vps20^{G2A}$. CPS is synthesized as a transmembrane precursor (pro-CPS) and is transported through the MVB pathway into the lumen of the vacuole. When exposed to the hydrolytic content of the vacuole, pro-CPS is proteolytically cleaved at the membrane, thereby releasing the soluble mature active enzyme. The transport and sorting of CPS into the vacuolar lumen can be followed by fusing the green fluorescent protein GFP to the cytoplasmic tail of CPS (Odorizzi et al., 1998). When wild-type cells expressing GFP-CPS are examined by fluorescence microscopy, GFP is detected within the vacuolar lumen (Figure 3B). In contrast, cells expressing $Vps20^{G2A}$ partially mislocalized GFP-CPS to the limiting vacuolar membrane. However, this trafficking defect was less severe than observed in the *vps20*Δ strain (Figure 3B). In summary, the simplest interpretation of our data would be that myristoylation of Vps20 is necessary for efficient sorting of endosomal cargo through the MVB sorting pathway and seems to play an important role in the membrane association and formation of ESCRT-III.

Proteolytic Processing of MVB Cargo Is Altered in ESCRT-III Mutants

Immunofluorescence microscopy indicated that ESCRT-III is localized to endosomes and is therefore in proximity to endosomal MVB cargo proteins. This prediction was tested by analyzing the localization of the ESCRT-III subunit Snf7 and the MVB cargo protein GFP-CPS by immunogold electron microscopy of yeast cells deleted for *VPS4*. These mutant cells accumulate ESCRT-III and cargo at an aberrant endosomal structure, the class E compartment (Babst et al., 1998). Single-label experiments showed that the MVB cargo GFP-CPS is highly concentrated in the multilamellar membranes of the class E compartment (Figure 4C). Single-label experiments also showed that Snf7 is also found on the multilamellar membranes that make up the class E compartment, as well as on vesicular structures immediately adjacent to the class E compartment (Figures 4A and 4B). While labeling for Snf7 in wild-type cells showed only a highly disperse cytoplasmic distribution (data not shown), it can be clearly seen that the vast majority of

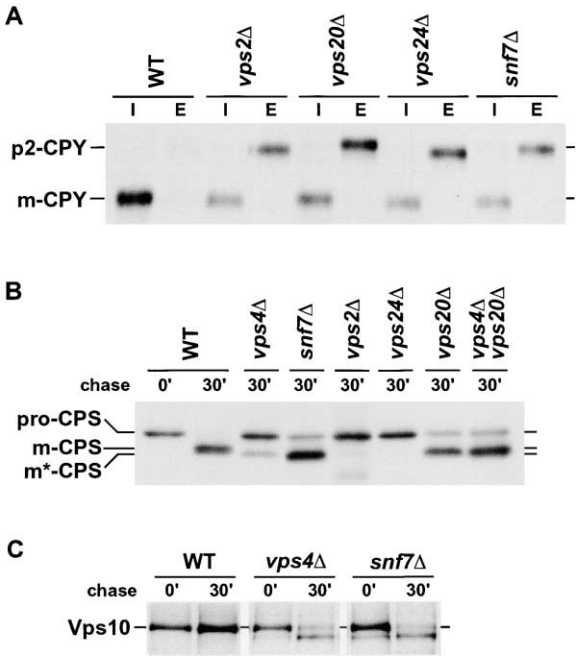

Figure 5. Formation of the Vps20-Snf7 Subcomplex Inhibits Proteolytic Clipping of the MVB Cargo CPS but Does Not Affect Clipping of Other Endosomal Cargo Such as CPY and Vps10

Yeast cells were labeled with Tran^{35}S-label for 10 min and lysed at indicated time points after adding chase. The proteolytic clipping of newly synthesized CPY, CPS, and Vps10 was monitored by immunoprecipitation and SDS-PAGE.

(A) To demonstrate mislocalization of CPY in all class E mutants, labeled yeast cells were separated for the immunoprecipitation analysis into intracellular (I) and extracellular (E) fractions.

(B) Protection of the MVB cargo CPS from clipping in mutants where the Vps20-Snf7 subcomplex has formed is revealed by pulse-chase immunoprecipitation of CPS from the indicated strains.

(C) Vps10 clipping is demonstrated by pulse-chase analysis from the indicated strains.

Snf7 localizes to the class E compartment in *vps4*Δ cells (Figures 4A and 4B). Using 5 nm gold particles to detect GFP-CPS and 10 nm gold particles to detect Snf7 in double-label experiments, it can be seen that both molecules are localized to multiple membranes of the class E compartment (Figure 4D). The distribution of cargo and machinery throughout the multilamellar structure of the class E compartment is consistent with the predicted colocalization of ESCRT-III and MVB cargo.

In class E *vps* mutants, the accumulation of cargo proteins such as hydrolases and the vacuolar ATPase in the class E compartment results in acidification of the compartment and activation of the hydrolytic enzymes. As a consequence, in the intracellular pool, the newly synthesized soluble vacuolar hydrolase CPY is proteolytically matured in the aberrant endosome, with kinetics similar to the maturation observed in the vacuoles of wild-type cells (Figure 5A). Furthermore, class E *vps* mutants secrete part of the newly synthesized CPY in its precursor form (p2-CPY; Figure 5A). Similarly, it has been described that membrane-associated pro-CPS is cleaved in the class E compartment (Babst et al., 2000). However, the resulting mature form of CPS (m*-CPS) is slightly smaller than m-CPS observed in wild-type cells, suggesting that the proteolytic clipping of pro-CPS occurs at a slightly different site within CPS in the endosome from that observed in the vacuolar lumen. Interestingly, pulse-chase experiments revealed that different class E *vps* mutants exhibit different maturation kinetics of newly synthesized pro-CPS. Class E *vps* mutants, which accumulated Vps20-Snf7 on the endosome (e.g., *vps2*Δ, *vps24*Δ, and *vps4*Δ), did not mature pro-CPS within 30 min of chase, whereas mutations that blocked Vps20-Snf7 complex formation (e.g., *snf7*Δ, *vps20*Δ, and *vps4*Δ*vps20*Δ) efficiently matured pro-CPS to m*-CPS (Figure 5B). This observation suggested that formation of the Vps20-Snf7 subcomplex on the endosome in some way reduces the accessibility of the pro-CPS clipping site to lumenal proteases.

The transmembrane sorting receptor for CPY, Vps10, trafficks between Golgi and endosomes and thereby functions to sort soluble hydrolases to the vacuole (Cooper and Stevens, 1996; Marcusson et al., 1994). In class E *vps* mutants, the lumenal domain of Vps10 is proteolytically clipped and the protein is rapidly degraded (Cereghino et al., 1995; Cooper and Stevens, 1996). This instability of Vps10 is not only observed in mutants blocking Vps20-Snf7 formation (e.g., *snf7*Δ, Figure 5C) but also in mutant cells that accumulate the Vps20-Snf7 complex on the endosome (e.g., *vps4*Δ, Figure 5C), which suggested that formation of Vps20-Snf7 specifically affects the proteolytic clipping of CPS, a cargo of the MVB pathway, but not all endosomal cargoes.

Discussion

Multivesicular bodies have been implicated in receptor trafficking and downregulation for more than 20 years (Gorden et al., 1978). However, the molecular machinery required for the formation of these late endosomal compartments has only recently begun to be characterized. Here, we characterize the ESCRT-III protein complex containing the class E Vps proteins Vps2, Vps24, Vps20, and Snf7. This protein complex transiently oligomerizes on the cytoplasmic face of the endosome during its required function in MVB formation.

Structure and Formation of ESCRT-III

The four class E Vps proteins, Vps24, Snf7, and the newly identified Vps2 and Vps20 are small, highly charged proteins containing one or two predicted coiled-coil domains (Figure 1). In wild-type cells, the bulk of these four small coiled-coil proteins are monomeric and localized to the cytoplasm. From the cytoplasm, the coiled-coil proteins are recruited to an endosomal membrane where they assemble into the protein complex ESCRT-III (Figure 2). The ESCRT-III membrane-associated protein complex seems to be composed of numerous subunits (Babst et al., 1998). Our studies suggested that ESCRT-III has a defined subunit stoichiometry and contains a similar number of each of the four coiled-coil proteins. However, because of the apparent large size of the protein complex, we were not able to determine whether ESCRT-III contains a defined number of subunits.

Vps2 and Vps24 are homologs, as are Vps20 and Snf7. Interestingly, these two pairs of homologous proteins

form two subcomplexes within ESCRT-III. The Vps20-Snf7 subcomplex is required for the membrane association of ESCRT-III. Furthermore, Vps20 contains a recognition sequence for the *N*-myristoyltransferase Nmt1, which during translation covalently attaches myristate to the N-terminal glycine of target proteins. It has been demonstrated that the N terminus of Vps20 is myristoylated in vitro, strongly suggesting that this is also the case in yeast cells (Ashrafi et al., 1998). We found that mutation of the N-terminal glycine of Vps20 resulted in partial loss of function and reduced membrane association of the protein (Figures 2 and 3). Therefore, myristoylation of Vps20 appears to play an important role for the proper localization and binding of ESCRT-III to the endosomal membrane and suggests that the Vps20-Snf7 subcomplex directly interacts with the lipids of the endosomal membrane. Although no obvious site for fatty acid modifications can be found in Snf7, it also has the ability to associate with endosomes, even in the absence of Vps20. Therefore, one possibility is that the highly charged Snf7 protein binds to membranes through interactions with charged lipid head groups.

The AAA-type ATPase Vps4 dissociates ESCRT-III from the endosomal membrane in an ATP-dependent manner. The recruitment of Vps4 to the endosome requires its N-terminal coiled-coil domain and depends on the presence of Vps2 and Vps24 on the endosomal membrane (Figure 3; Babst et al., 1998). Consistent with this, we found that deletion of Vps2 or Vps24 resulted in accumulation of the Vps20-Snf7 subcomplex on membranes. Together, the data suggest that Vps4 binds to ESCRT-III via coiled-coil interaction with the Vps2-Vps24 subcomplex and that this interaction is necessary for the Vps4-dependent dissociation of ESCRT-III.

Efficient sorting of certain cargo into the MVB pathway is dependent on ubiquitination of the cytoplasmic domain of these proteins. Another class E Vps protein complex, ESCRT-I, binds to the ubiquitin-tagged cargo and initiates the sorting reaction (Katzmann et al., 2001). However, these studies also indicated that prior to entry into the MVB vesicles, the ubiquitin tag is removed from the cargo by the deubiquitinating enzyme. This is consistent with previous data in which cells deleted for *DOA4* were shown to deliver ubiquitinated endosomal proteins to the vacuolar lumen, resulting in the degradation of ubiquitin along with cargo (Swaminathan et al., 1999). Doa4 localizes to endosomal membranes and proper localization of Doa4 requires the Vps24 protein (Amerik et al., 2000). These observations suggest that, like Vps4, Doa4 associates with the endosome through an interaction with the Vps2-Vps24 subcomplex of ESCRT-III. By this model, the interaction with ESCRT-III localizes Doa4 to its proper site of function, where it plays an important role in the efficient deubiquitination of cargo and the recycling of ubiquitin molecules.

Two genes have been described, *VPS60/MOS10* (SGD, YDR486C) and *DID2/FTI1* (SGD, YKR035W-A), which encode small hydrophilic coiled-coil proteins that share homology with the genes encoding the ESCRT-III subunits (Amerik et al., 2000; Kranz et al., 2001). Phenotypic analysis of *VPS60* and *DID2* deletion strains demonstrated that these two genes indeed belong to the group of class E *VPS* genes. These data could suggest that Vps60 and Did2 are additional subunits of ESCRT-III. However, we found that the trafficking defects of *vps60*Δ and *did2*Δ cells are less severe than in strains deleted for one of the four ESCRT-III subunits and that ESCRT-III membrane association was not blocked in these mutants, suggesting that Vps60 and Did2 function is partially redundant or that these two proteins might play a regulatory role in ESCRT-III activity (data not shown).

ESCRT-III Functions in Sorting of MVB Cargo

The vacuolar hydrolase CPS is synthesized as a transmembrane precursor which is matured by proteolytic clipping at a site on the lumenal side of the membrane (Spormann et al., 1992). In wild-type cells, this maturation event occurs after the sorting of CPS via the MVB pathway into the vacuolar lumen. However, class E *vps* mutants are defective in the transport of CPS and other newly synthesized vacuolar hydrolases. Many of these hydrolases accumulate in the prevacuolar class E compartment, where they are matured to their active forms. Interestingly, we found that the kinetics of endosomal maturation of pro-CPS was influenced by the presence of the Vps20-Snf7 subcomplex on the endosomal membrane. Class E *vps* mutants which accumulate Vps20-Snf7 on the endosome (e.g., *vps4*Δ, *vps2*Δ, and *vps24*Δ) mature pro-CPS with very slow kinetics, while mutant cells which impair Vps20-Snf7 function (e.g., *vps20*Δ, *snf7*Δ, and *vps4*Δ*vps20*Δ) mature pro-CPS with rapid (wild-type) kinetics (Figure 5). In contrast, proteolytic clipping of endosomal cargo which is not subject to MVB sorting, such as the soluble hydrolase CPY or the transmembrane CPY sorting receptor Vps10, takes place in all class E mutants, regardless of the accumulation of the Vps20-Snf7 complex on endosomal membranes. These data indicate that the endosome-associated Vps20-Snf7 complex reduces the accessibility of the MVB cargo pro-CPS to soluble proteases. This could result from either (1) steric hindrance of protease accessibility caused by cargo concentration or (2) the sorting of pro-CPS into a subcompartment of the endosome where soluble hydrolases have limited access. In either case, the data suggest a direct role of the Vps20-Snf7 complex in the sorting of MVB cargo, possibly by transient interactions between Vps20-Snf7 and specific MVB cargo. This model is supported by the observation that Doa4, which functions in the deubiquitination of MVB cargo, is localized in proximity to its substrate by binding to ESCRT-III (Amerik et al., 2000).

Model for the Function of the ESCRT Protein Complexes

The class E Vps proteins and protein complexes are localized mainly to the cytoplasm and are transiently recruited to endosomal compartments in order to execute the sorting of endosomal cargo and the formation of MVBs. ESCRT-III appears to represent the central, core apparatus of the class E Vps sorting machinery. Based on the present and previously published data, we propose the following working model for the ESCRT machinery in the MVB sorting pathway (Figure 6). ESCRT-I binds to ubiquitinated endosomal cargo, such as the newly synthesized vacuolar hydrolase pro-CPS (Katzmann et al., 2001). By an as yet unclear mechanism,

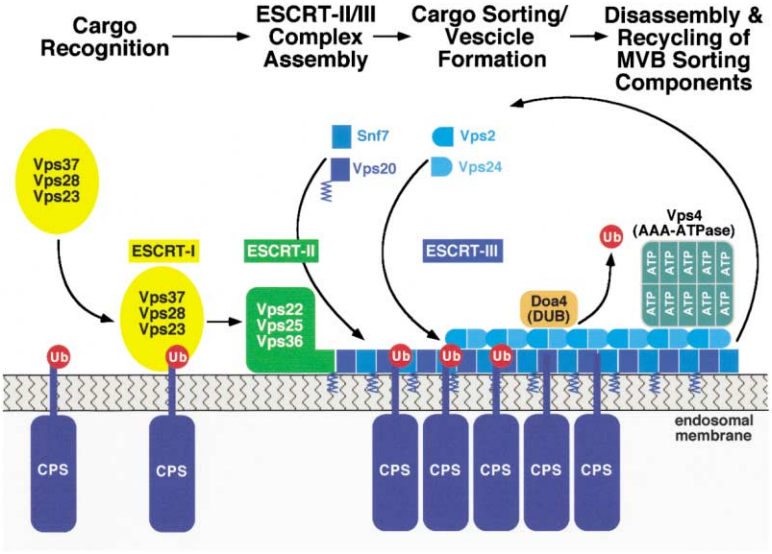

Figure 6. Model for the MVB Sorting of Ubiquitinated Endosomal Cargo by the Class E Vps Protein Machinery

At the endosome, ubiquitinated CPS is recognized by ESCRT-I, which then activates ESCRT-II function in the recruitment and oligomerization of the small coiled-coil proteins to form ESCRT-III. The ESCRT-III protein complex sorts and concentrates CPS into a subdomain of the endosome that then invaginates to form a vesicle. The deubiquitinating (DUB) enzyme Doa4 binds to ESCRT-III and thereby removes the ubiquitin tag from the cargo prior to entry into the MVB vesicle. After completion of MVB sorting, the AAA-type ATPase Vps4 is recruited to ESCRT-III, which results in the dissociation of the protein complex from the membrane.

we propose that ESCRT-I activates endosomal ESCRT-II. Active ESCRT-II then binds to the myristoylated coiled-coil protein Vps20 and thereby initiates the recruitment of Vps20 and Snf7 to the endosome and the oligomerization of these coiled-coil proteins into the Vps20-Snf7 membrane-associated subcomplex. The formation of ESCRT-III is completed by the addition of the Vps2-Vps24 subcomplex. It is likely that additional class E proteins transiently associate with the core ESCRT complexes. For instance, the class E Vps protein Vps27/Hrs has been shown to interact with both ubiquitin and the endosomal lipid phosphatidylinositol 3-phosphate and therefore is likely to act with the ESCRT machinery (Raiborg et al., 2002; Shih et al., 2002). The formation of the ESCRT structure on the cytoplasmic face of the endosome results in sorting and concentration of the ubiquitinated cargo destined for the MVB pathway, possibly by interacting with the cytoplasmic domains of the cargo and/or by restricting the MVB cargo within a subdomain of the endosomal membrane. Doa4 is recruited by ESCRT-III in order to recycle the ubiquitin molecule from ubiquitin-tagged MVB cargoes after the initial ubiquitin-dependent sorting is completed, presumably resulting in commitment to entry into the MVB vesicles. Finally, after completion of cargo sorting and MVB vesicle formation, the AAA-type ATPase Vps4 is recruited by ESCRT-III, where it catalyzes the disassembly and dissociation of the complex, resulting in the recycling of the class E Vps proteins into the cytoplasm for further rounds of MVB sorting.

Table 1. Strains and Plasmids Used in this Study

Strain or plasmid	Descriptive name	Genotype or description	Reference or source
S. cerevisiae			
SEY6210	WT	*MAT*α *leu2-3,112 ura3-52 his3-*Δ*200 trp1-*Δ*901 lys2-801 suc2-*Δ*9*	(Robinson et al., 1988)
MBY28	*vps2*Δ	SEY6210; *vps2*Δ*1* (*VPS2::HIS3*)	This study
MBY3	*vps4*Δ	SEY6210; *vps4*Δ*1* (*VPS4::TRP1*)	(Babst et al., 1997)
EEY2-1	*vps20*Δ	SEY6210; *vps20*Δ*1* (*VPS20::HIS3*)	This study
BWY102	*vps24*Δ	SEY6210; *vps24*Δ*1* (*VPS24::HIS3*)	(Babst et al., 1998)
EEY9	*snf7*Δ	SEY6210; *snf7*Δ*1* (*SNF7::HIS3*)	This study
MBY41	*vps4*Δ*vps2*Δ	SEY6210; *vps4*Δ*1* (*VPS4::TRP1*), *vps2*Δ*1* (*VPS2::HIS3*)	This study
MBY37	*vps4*Δ*vps20*Δ	SEY6210; *vps4*Δ*1* (*VPS4::TRP1*), *vps20*Δ*1* (*VPS20:HIS3*)	This study
MBY12	*vps4*Δ*vps24*Δ	SEY6210; *vps4*Δ*1* (*VPS4::TRP1*), *vps24*Δ*1* (*VPS24::HIS3*)	This study
EEY12	*vps4*Δ*snf7*Δ	SEY6210; *vps4*Δ*1* (*VPS4::TRP1*), *snf7*Δ*1* (*SNF7::HIS3*)	This study
E. coli			
XL1-blue		*recA1 endA1 gyrA96 thi-1 hsdR17 supE44 relA1 lac* [F′ *proAB lacI*^{q}*Z*Δ*M15* Tn*10*(tet^r)]	Stratagene
Plasmids			
pRS416		*URA3* Ap^R *CEN*	(Christianson et al., 1992)
pGEX-2T		Ap^R	Amersham Pharmacia Biotech
pGO45	GFP-CPS	*URA3* Ap^R (pRS426) *GFP-CPS1*	(Odorizzi et al., 1998)
pMB149	*vps4-HA*^{E233Q}	*URA3* Ap^R (pRS416) *vps4-HA*^{E233Q}	This study
pMB160	GST-SNF7	Ap^R (pGEX-2T) *GST-SNF7*	This study
pMB167	*VPS2-HA*	*URA3* Ap^R (pRS416) *VPS2-HA*	This study
pMB168	*VPS20-HA*	*URA3* Ap^R (pRS416) *VPS20-HA*	This study
pMB172	(His)$_6$-SNF7	*URA3* Ap^R (pRS416) *(His)$_6$-SNF7*	This study
pMB176	*vps20-HA*^{G2A}	*URA3* Ap^R (pRS416) *vps20-HA*^{G2A}	This study

Several mammalian homologs of yeast class E Vps proteins have been identified and analyses have indicated that the function of these proteins is conserved among all eukaryotes (Babst et al., 2000; Bishop and Woodman, 2000, 2001; Yoshimori et al., 2000). Therefore, we suggest that in mammalian cells, the ubiquitination of endocytic and biosynthetic cargo also serves as a sorting signal for ESCRT-dependent delivery of these cargo proteins into the lysosomal lumen. This idea is supported by studies which have shown that efficient downregulation and degradation of the activated cell surface receptor EGFR (epidermal growth factor receptor) involves the ubiquitination of the cytoplasmic tail of the activated receptor by the ubiquitin ligase c-Cbl (reviewed in Waterman and Yarden, 2001). The data suggest that ubiquitination of endocytosed cargo redirects the proteins from the recycling pathway into MVB vesicles and therefore marks these cargo molecules for lysosomal/vacuolar degradation. As a consequence, the ubiquitin-dependent sorting into the MVB pathway might not only regulate the stability of certain activated cell surface receptors but may also regulate the turnover of misfolded or abnormal membrane proteins. Further study will be required to address a possible role for the ESCRT machinery in membrane protein quality control. Furthermore, additional biochemical studies will be necessary to determine the precise role of the ESCRT machinery in the combined processes of cargo sorting and the unique mechanism of MVB vesicle formation. Among vesicle formation events this mechanism is unique in that it is directed toward the lumen of the compartment, rather than the cytosol. Interestingly, the topology of this budding event mimics that of viral particle formation at the plasma membrane which, in the case of HIV-1, has recently been shown to utilize class E Vps protein function (Garrus et al., 2001).

Experimental Procedures

Materials

Monoclonal antibodies specific for the HA (hemagglutinin) epitope were purchased from Boehringer Mannheim. Polyclonal antiserum against Snf7 (Babst et al., 1998), Vps24 (Babst et al., 1998), CPY (Robinson et al., 1988), Vps10 (Marcusson et al., 1994), and CPS (Cowles et al., 1997) has been characterized previously.

Strains and Media

S. cerevisiae and *E. coli* strains used in this work are listed in Table 1. Yeast strains were grown in standard yeast extract-peptone-dextrose (YPD) or synthetic medium supplemented with essential amino acids as required for maintenance of plasmids (YNB; Sherman et al., 1979). Luria-Bertani (LB) medium was used for growth of *E. coli* cells (Miller, 1972). For selection of plasmids, 100 μg ml^{-1} ampicillin was added to the media.

The mutant strains MBY28, EEY2-1, and EEY9-1 were constructed by transforming SEY6210 wild-type strain with a DNA fragment containing the *HIS3* gene flanked by 50 bp specific for the upstream and downstream regions of the corresponding gene. The double mutants MBY41, MBY37, MBY12, and EEY12 were constructed by transforming the single *HIS3* marked knockouts with a DNA fragment containing the *TRP1* gene flanked by ~200 bp *VPS4* upstream and downstream DNA (*vps4Δ1*). Yeast cells were selected for the presence of the *TRP1* or *HIS3* gene and the deletions were confirmed by PCR analysis of the chromosomal DNA.

DNA Manipulations

Recombinant DNA work was performed using standard protocols (Sambrook et al., 1989). Transformation of *S. cerevisiae* was done by the lithium acetate method as described (Ito et al., 1983). The plasmids used in this study are listed in Table 1. The plasmid pMB149 was constructed by inserting the EcoRI/SalI fragment of pMB96 (Babst et al., 1998) into pRS416. To construct the *GST-SNF7* fusion, a PCR product containing the *SNF7* gene was ligated with the SmaI/SalI-digested expression vector pGEX-2T (Amersham Pharmacia Biotech), resulting in pMB160. For the construction of pMB167 and pMB168, a DNA fragment coding for three HA epitopes was ligated with PCR products containing either *VPS2* or *VPS20*, respectively, and inserted into SalI/SpeI-digested pRS416 vector. The plasmid pMB176 was obtained by a PCR-based point mutagenesis of pMB168 resulting in the codon exchange of the position 2 glycine to an alanine. This mutation was confirmed by DNA sequencing. In order to construct the *(His)$_6$-SNF7* fusion, a PCR product containing *SNF7* was inserted into the NdeI/BamHI-digested expression vector pET-15b (Novagen). The resulting plasmid was digested with NcoI/BamHI and ligated with a NotI/NcoI-digested PCR product, containing the CPS promoter region, into pRS416 digested with BamHI/NotI, resulting in the plasmid pMB172.

Biochemical Assays

Bacterially expressed GST-Snf7 was purified and cleaved with thrombin as described (Babst et al., 1997). Wild-type yeast cells expressing *(His)$_6$-SNF7* (SEY6210 pMB172) were spheroplasted and lysed in PBS (8 g/l NaCl, 0.2 g/l KCl, 1.44 g/l Na_2HPO_4, 0.24 g/l KH_2PO_4 [pH 7.2]) containing AEBSF (Calbiochem-Novabiochem) and protease inhibitor cocktail (Complete; Roche Molecular Biochemicals). To purify the $(His)_6$-Snf7 fusion protein, the cell lysate was subjected to Ni^{2+} affinity chromatography according to manufacturer's protocol (His-Bind Resin; Novagen). Subcellular fractionation and Western blot analyses were performed as previously described (Babst et al., 1997).

For native immunoprecipitation experiments, 10 OD_{600} equivalents of yeast cells were spheroplasted, osmotically lysed in 1 ml PBS containing protease inhibitors, and the resulting cell extracts were centrifuged at 15,000 $\times$ g for 5 min. The pellet fraction was resuspended in 0.2 ml PBS containing protease inhibitors and 1% Triton X-100 and incubated for 10 min on ice. 0.8 ml PBS was added and the solubilized membrane fractions were centrifuged at 15,000 $\times$ g for 5 min. The resulting supernatant was incubated with antibodies (1/250 polyclonal antiserum, 1.5 μg/ml monoclonal antibody) for 1.5 hr at 4°C. The antibodies were isolated by adding either protein A Sepharose CL-4B (Amersham Pharmacia Biotech) for polyclonal antibodies or GammaBind G Sepharose (Amersham Pharmacia Biotech) for monoclonal antibodies. After incubation for 1 hr at 4°C, the Sepharose was washed three times with PBS containing 0.5% Tween-20, and the antibodies together with the bound antigen were eluted by boiling the Sepharose in SDS-PAGE sample buffer. The resulting fractions were analyzed by SDS-PAGE and Western blotting.

Microscopy and Pulse-Chase Experiments

Immunofluorescence microscopy was performed on fixed spheroplasted cells as described (Babst et al., 1998). Pulse-chase experiments were performed either on whole cells (CPS, Vps10) or in the case of CPY trafficking studies, on spheroplasted cells, which allowed us to differentiate between intracellular and extracellular localization of CPY. The ^{35}S-labeled proteins were analyzed by immunoprecipitation and SDS-PAGE (Rieder et al., 1996).

For immunoelectron microscopy, cells were processed essentially as previously described (Reider et al., 96). Primary antibodies against GFP (monoclonal MMS-118P, clone B34, Covance Research Products) and Snf7 (Babst et al., 1998) were diluted 1/100 and 1/1000, respectively. Incubation with primary antibodies for 1 hr at room temperature was followed by gold-conjugated goat anti-mouse IgG and IgM (Amersham Pharmacia Biotech) and gold-conjugated goat anti-rabbit IgG, both diluted 1/25 in 1% BSA/PBS at room temperature for 30 min. Grids were viewed and photographed using a JEOL 1200EX II transmission electron microscope (JEOL).

Acknowledgments

We wish to thank Drs. Chris Stefan and Tamara Darsow for critical reading of the manuscript and members of the Emr lab for constructive comments. We would also like to thank Dr. Marian Carlson for

useful discussions. T.M. is a member of Immunoelectron Microscopy core B, program project grant CA58689, headed by M. Farquhar. This work was supported by a grant from the NIH to S.D.E. (CA58689), a fellowship from the Howard Hughes Medical Institute (M.B.), and a fellowship from the American Cancer Society (D.J.K.). S.D.E. is supported as an Investigator of the Howard Hughes Medical Institute.

Received: January 7, 2002
Revised: June 3, 2002

References

Amerik, A.Y., Nowak, J., Swaminathan, S., and Hochstrasser, M. (2000). The Doa4 deubiquitinating enzyme is functionally linked to the vacuolar protein-sorting and endocytic pathways. Mol. Biol. Cell *11*, 3365–3380.

Ashrafi, K., Farazi, T.A., and Gordon, J.I. (1998). A role for *Saccharomyces cerevisiae* fatty acid activation protein 4 in regulating protein N-myristoylation during entry into stationary phase. J. Biol. Chem. *273*, 25864–25874.

Babst, M., Sato, T.K., Banta, L.M., and Emr, S.D. (1997). Endosomal transport function in yeast requires a novel AAA-type ATPase, Vps4p. EMBO J. *16*, 1820–1831.

Babst, M., Wendland, B., Estepa, E.J., and Emr, S.D. (1998). The Vps4p AAA ATPase regulates membrane association of a Vps protein complex required for normal endosome function. EMBO J. *17*, 2982–2993.

Babst, M., Odorizzi, G., Estepa, E.J., and Emr, S.D. (2000). Mammalian tumor susceptibility gene 101 (TSG101) and the yeast homologue, Vps23p, both function in late endosomal trafficking. Traffic *1*, 248–258.

Babst, M., Katzmann, D.J., Snyder, W.B., Wendland, B., and Emr, S.D. (2002). Endosome-associated complex, ESCRT-II, recruits transport machinery for protein sorting at the multivesicular bodies. Dev. Cell *3*, this issue, 283–289.

Bishop, N., and Woodman, P. (2000). ATPase-defective mammalian VPS4 localizes to aberrant endosomes and impairs cholesterol trafficking. Mol. Biol. Cell *11*, 227–239.

Bishop, N., and Woodman, P. (2001). Tsg101/mammalian vps23 and mammalian vps28 interact directly and are recruited to vps4-induced endosomes. J. Biol. Chem. *276*, 11735–11742.

Cereghino, J.L., Marcusson, E.G., and Emr, S.D. (1995). The cytoplasmic tail domain of the vacuolar sorting receptor Vps10p and a subset of *VPS* gene products regulate receptor stability, function and localization. Mol. Biol. Cell *6*, 1089–1102.

Christianson, T.W., Sikorski, R.S., Dante, M., Shero, J.H., and Hieter, P. (1992). Multifunctional yeast high-copy-number shuttle vectors. Gene *110*, 119–122.

Cooper, A.A., and Stevens, T.H. (1996). Vps10p cycles between the late-Golgi and prevacuolar compartments in its function as the sorting receptor for multiple yeast vacuolar hydrolases. J. Cell Biol. *133*, 529–541.

Cowles, C.R., Snyder, W.B., Burd, C.G., and Emr, S.D. (1997). An alternative Golgi to vacuole delivery pathway in yeast: identification of a sorting determinant and required transport component. EMBO J. *16*, 2769–2782.

Felder, S., Miller, K., Moehren, G., Ullrich, A., Schlessinger, J., and Hopkins, C.R. (1990). Kinase activity controls the sorting of the epidermal growth factor receptor within the multivesicular body. Cell *61*, 623–634.

Futter, C.E., Pearse, A., Hewlett, L.J., and Hopkins, C.R. (1996). Multivesicular endosomes containing internalized EGF-EGF receptor complexes mature and then fuse directly with lysosomes. J. Cell Biol. *132*, 1011–1023.

Garrus, J.E., von Schwedler, U.K., Pornillos, O.W., Morham, S.G., Zavitz, K.H., Wang, H.E., Wettstein, D.A., Stray, K.M., Cote, M., Rich, R.L., et al. (2001). Tsg101 and the vacuolar protein sorting pathway are essential for HIV-1 budding. Cell *107*, 55–65.

Gorden, P., Carpentier, J.L., Cohen, S., and Orci, L. (1978). Epidermal growth factor: morphological demonstration of binding, internalization, and lysosomal association in human fibroblasts. Proc. Natl. Acad. Sci. USA *75*, 5025–5029.

Hicke, L. (1997). Ubiquitin-dependent internalization and down-regulation of plasma membrane proteins. FASEB J. *11*, 1215–1226.

Ito, H., Fukuda, Y., Murata, K., and Kimura, A. (1983). Transformation of intact yeast cells treated with alkali cations. J. Bacteriol. *153*, 163–168.

Katzmann, D.J., Babst, M., and Emr, S.D. (2001). Ubiquitin-dependent sorting into the multivesicular body pathway requires the function of a conserved endosomal protein sorting complex, ESCRT-I. Cell *106*, 145–155.

Kranz, A., Kinner, A., and Kolling, R. (2001). A family of small coiled-coil-forming proteins functioning at the late endosome in yeast. Mol. Biol. Cell *12*, 711–723.

Lemmon, S.K., and Traub, L.M. (2000). Sorting in the endosomal system in yeast and animal cells. Curr. Opin. Cell Biol. *12*, 457–466.

Marcusson, E.G., Horazdovsky, B.F., Cereghino, J.L., Gharakhanian, E., and Emr, S.D. (1994). The sorting receptor for yeast vacuolar carboxypeptidase Y is encoded by the *VPS10* gene. Cell *77*, 579–586.

Miller, J. (1972). Experiments in Molecular Genetics (Cold Spring Harbor, NY: Cold Spring Harbor Laboratory Press).

Odorizzi, G., Babst, M., and Emr, S.D. (1998). Fab1p PtdIns(3)P 5-kinase function essential for protein sorting in the multivesicular body. Cell *95*, 847–858.

Piper, R.C., Cooper, A.A., Yang, H., and Stevens, T.H. (1995). *VPS27* controls vacuolar and endocytic traffic through a prevacuolar compartment in *Saccharomyces cerevisiae*. J. Cell Biol. *131*, 603–618.

Raiborg, C., Bache, K.G., Gillooly, D.J., Madshus, I.H., Stang, E., and Stenmark, H. (2002). Hrs sorts ubiquitinated proteins into clathrin-coated microdomains of early endosomes. Nat. Cell Biol., in press.

Raymond, C.K., Howald-Stevenson, I., Vater, C.A., and Stevens, T.H. (1992). Morphological classification of the yeast vacuolar protein sorting mutants: evidence for a prevacuolar compartment in class E *vps* mutants. Mol. Biol. Cell *3*, 1389–1402.

Reggiori, F., and Pelham, H.R. (2001). Sorting of proteins into multivesicular bodies: ubiquitin-dependent and -independent targeting. EMBO J. *20*, 5176–5186.

Rieder, S.E., Banta, L.M., Kohrer, K., McCaffery, J.M., and Emr, S.D. (1996). Multilamellar endosome-like compartment accumulates in the yeast *vps28* vacuolar protein sorting mutant. Mol. Biol. Cell *7*, 985–999.

Robinson, J.S., Klionsky, D.J., Banta, L.M., and Emr, S.D. (1988). Protein sorting in *Saccharomyces cerevisiae*: isolation of mutants defective in the delivery and processing of multiple vacuolar hydrolases. Mol. Cell. Biol. *8*, 4936–4948.

Sambrook, J., Fritsch, E.F., and Maniatis, T. (1989). Molecular Cloning: A Laboratory Manual, Second Edition (Cold Spring Harbor, NY: Cold Spring Harbor Laboratory Press).

Scheuring, S., Bodor, O., Rohricht, R.A., Muller, S., Beyer, A., and Kohrer, K. (1999). Cloning, characterisation, and functional expression of the *Mus musculus* SKD1 gene in yeast demonstrates that the mouse SKD1 and the yeast VPS4 genes are orthologues and involved in intracellular protein trafficking. Gene *234*, 149–159.

Sherman, F., Fink, G.R., and Lawrence, L.W. (1979). Methods in Yeast Genetics: A Laboratory Manual (Cold Spring Harbor, NY: Cold Spring Harbor Laboratory Press).

Shih, S.C., Katzmann, D.J., Schnell, J.D., Sutanto, M., Emr, S.D., and Hicke, L. (2002). Epsins and Vps27/Hrs contain ubiquitin-binding domains that function in receptor endocytosis and downregulation. Nat. Cell Biol., in press.

Sorkin, A. (1998). Endocytosis and intracellular sorting of receptor tyrosine kinases. Front. Biosci. *3*, D729–D738.

Spormann, D.O., Heim, J., and Wolf, D.H. (1992). Biogenesis of the yeast vacuole (lysosome). The precursor forms of the soluble hydrolase carboxypeptidase yscS are associated with the vacuolar membrane. J. Biol. Chem. *267*, 8021–8029.

Swaminathan, S., Amerik, A.Y., and Hochstrasser, M. (1999). The

Doa4 deubiquitinating enzyme is required for ubiquitin homeostasis in yeast. Mol. Biol. Cell *10*, 2583–2594.

van Deurs, B., Holm, P.K., Kayser, L., Sandvig, K., and Hansen, S.H. (1993). Multivesicular bodies in HEp-2 cells are maturing endosomes. Eur. J. Cell Biol. *61*, 208–224.

Waterman, H., and Yarden, Y. (2001). Molecular mechanisms underlying endocytosis and sorting of ErbB receptor tyrosine kinases. FEBS Lett. *490*, 142–152.

Yoshimori, T., Yamagata, F., Yamamoto, A., Mizushima, N., Kabeya, Y., Nara, A., Miwako, I., Ohashi, M., Ohsumi, M., and Ohsumi, Y. (2000). The mouse SKD1, a homologue of yeast Vps4p, is required for normal endosomal trafficking and morphology in mammalian cells. Mol. Biol. Cell *11*, 747–763.